JOURNAL OF MATERIALS SCIENCE 5 (1970) 1073-1077

Heteroepitaxial Growth of Si on $ZnSiP_2$

I. BERTÓTI
Research Institute for Technical Physics of the Hungarian Academy of Sciences, Budapest, Ujpest 1, POB 76

Silicon layers were deposited epitaxially on natural facets of solution-grown $ZnSiP_2$ crystals by hydrogen reduction of $SiHCl_3$. Orientation relationships between the diamond-structured layer and the chalcopyrite type substrate were determined giving the results: (112) $ZnSiP_2$ parallel to (111) Si and (101) $ZnSiP_2$ parallel to (201) Si. Structural and some electrical properties of the heterojunctions were investigated. Considerations concerning the misfit dislocations are presented.

1. Introduction

The crystallographic and semiconductor properties of $ZnSiP_2$ and other II-IV-V_2 type compounds have been widely studied [1-3]. Since the formation of p-n junctions proved to be difficult and the problem not yet solved, it is reasonable to approach it by the study of heterojunction combinations. However, only a few papers have been published on heterojunctions involving these compounds [4, 5]. Due to the great similarity between the calcopyrite-type lattice of $ZnSiP_2$ and the diamond-type lattice of Si, and the small difference between their lattice constants (for $ZnSiP_2$ $a = 5.400$ Å, $c = 10.440$ Å; for Si $a = 5.431$ Å) it was reasonable to choose the $ZnSiP_2$-Si pair for studying heteroepitaxy and heterojunction properties.

2. Experimental

2.1. Preparation and Morphology of $ZnSiP_2$ Substrates

The $ZnSiP_2$ substrate crystals were grown from Sn solution in vacuum-sealed silica ampoules. The melt containing 6 mole % $ZnSiP_2$ (added as elements) was cooled from the high temperature limit of the synthesis of 1200°C by a rate of 4.5°C/h, according to the data given in [1, 6]. The crystals obtained had a prismatic habit and were of about $8 \times 2 \times 1$ mm³ in volume. The crystallographic indices of the well developed faces were determined by optical goniometry and were identified by X-ray methods. The longitudinal axis of the crystals coincides with the $[\bar{1}\,\bar{1}\,1]$ tetragonal zone axis and the facets parallel to the latter are the (112), $(\bar{1}\,\bar{1}\,2)$, (101), $(\bar{1}0\bar{1})$, (011) and $(0\bar{1}\,\bar{1})$ planes. Small facets, most probably of (001) or (100) orientation were also found. Twinning parallel to (112) planes occurred in the majority of the crystals.

2.2. Growth of Epitaxial Si Layers

For growing Si layers the conventional hydrogen reduction of $SiHCl_3$ was applied. The substrates were etched in dilute $HCl:H_2O_2$ solution before deposition. The growth temperature of the layers was 1050 to 1150°C as determined on a pilot Si sample by optical pyrometry. For the applied gaseous mixture of $SiHCl_3:H_2 = 4.05 \times 10^{-3}$ mol/mol the average growth rate of the layers was 0.5 to 0.8 μm/min. Generally, the thickness of the layers was 5 to 10 μm. Under these conditions each of the exposed substrate planes was epitaxially covered by Si. Since under these growth conditions the substrates are subjected to strong thermal and chemical etching, until they are completely covered by Si, it seemed to be reasonable to apply rapid heating and a high growing rate.

3. Results

3.1. Orientation Relationships

In order to establish the epitaxial relationships, Laue back-reflection and glancing angle electron diffraction methods, and X-ray diffractometry (using Cu radiation) were applied. The layer orientations so determined were compared with the substrate orientation. To obtain additional information on the epitaxy, the layers were investigated by optical microscopy.

3.1.1. Layers on (112) $ZnSiP_2$ Planes

A characteristic triangular structure along the

<110> cubic directions was observed on the surface of silicon layers grown on (112) $ZnSiP_2$ planes (fig. 1). The typical three-fold symmetry suggested (111) layer orientation. This was proved by Laue patterns and by X-ray diffractograms. Laue patterns show three-fold symmetry with coinciding (112) and (111) reflections of the substrate and the layer, respectively. Diffractograms show peaks at angles corresponding to the spacing of (112) $ZnSiP_2$ and (111) Si lattice planes.

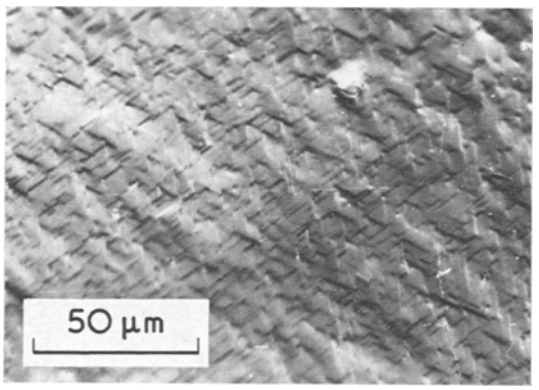

Figure 1 Surface structure of epitaxial Si layers grown on (112) $ZnSiP_2$ plane.

3.1.2. Layers on (101) $ZnSiP_2$ Planes

Si layers grown on (101) and (011) $ZnSiP_2$ planes exhibit more complex surface structure (fig. 2). Dark rows are often visible along the lines of intersections of emerging twin planes with the surface. Laue and glancing angle electron diffraction patterns (fig. 3) show two-fold symmetry with coinciding (101) $ZnSiP_2$ and (201) Si reflections, i.e. the (101) $ZnSiP_2$ parallel to (201) Si epitaxial relationship exists.

3.1.3. Layers Grown on Small Facets

Typical rectangular surface structure characteristic of the (100) Si orientation was found on the layer surfaces grown on the small tips and facets of the substrates. The exact orientation relationship could not be determined by the above methods because of the small dimensions of these surfaces.

3.2. Junction Properties

3.2.1. Structure of the Heterojunction

To obtain more complete data on the heterojunction interface, cross- and angle-lapped

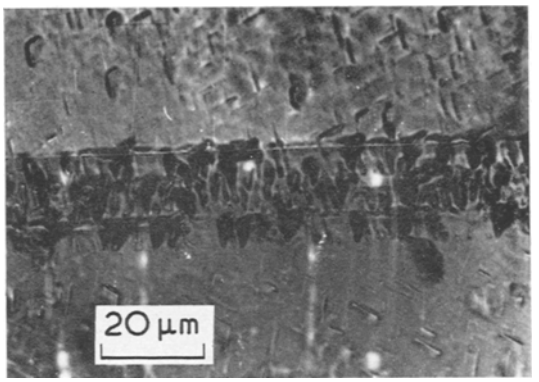

Figure 2 Surface structure of Si layer grown on (101) $ZnSiP_2$ plane.

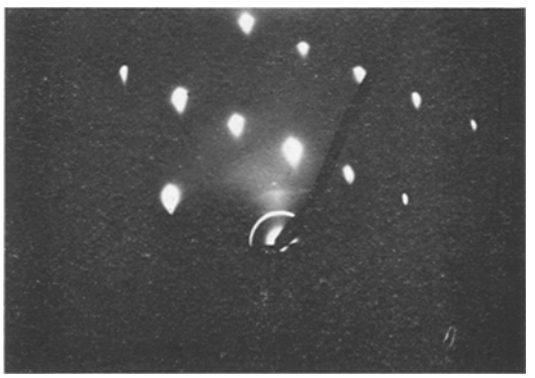

Figure 3 Glancing angle electron diffraction pattern of Si layer grown on (101) $ZnSiP_2$ plane.

sections of the samples were examined. As pointed out before, the substrates were subjected to strong thermal and chemical etching during the layer growth. This frequently causes hemispherically shaped pits on the substrate surface, detectable on angle-lapped sections, and also suggesting the occurrence of a liquid phase in the first stage of the growth process. After slight etching of the cross sections in $HCl:H_2O_2$ solution, revealing clearly the position of the interface, beside the intermediate layer, a new phase became visible in the form of small islands (fig. 4). The intermediate phase consisted of Si enriched in P, while the islands were found to be mainly SiP, as detected by electron probe microanalysis (EPMA) (fig. 5).

3.2.2. Electrical Properties

Heavily doped n-type layers were always formed on the solution-grown n-type substrates as

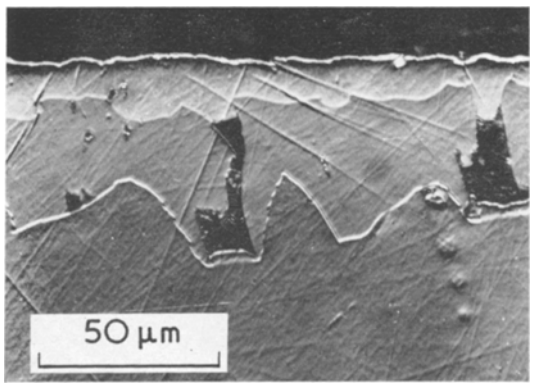

Figure 4 Cross-section of Si layer on $ZnSiP_2$ showing strong interaction and a wide intermediate layer between the deposit (above) and the substrate (below).

detected by the sign of thermal emf. Alloyed contacts were applied on both sides of the samples: Au to Si layers and In-Zn to the $ZnSiP_2$ substrates. Diode characteristics were detected on these heterostructures with a forward-to-reverse ratio of about 30 at 1.5 V bias for the best samples (fig. 6).

3.3. Misfit Considerations

The geometry of misfit dislocations has been developed and outlined for a number of heterojunction combinations with diamond and sphalerite structures [7]. Precautions must be taken, however, in applying this geometrical model for matching lattices of different crystal structures. Fortunately, the small tetragonal compression of $ZnSiP_2$ lattice probably does not impose a drastic distortion of the interface geometry and so the general model remains unchanged or needs to be slightly modified. Consequently, a net of misfit dislocations similar to a diamond-sphalerite type heterojunction can be deduced. In the case of (112) $ZnSiP_2$ ‖ (111) Si the number of dangling bonds will amount to $N_S = 2.7 \times 10^{13}$ cm^{-2}. Because of the tetragonal compression of $ZnSiP_2$ two sets of misfit lines will have equal repeat distances of 0.015 μm, measured in the $[10\bar{1}]$ and $[01\bar{1}]$ Burgers vector directions, and the third set of lines will have 0.067 μm, measured in the $[1\bar{1}0]$ Burgers vector direction. For (101) $ZnSiP_2$ ‖ (201) Si epitaxy, which represents a new relationship, a two dimensional drawing enabled us to determine the directions of misfit dislocations. According to this drawing the lines run in the [010] and $[10\bar{2}]$ cubic directions resulting in a rectangular grid.

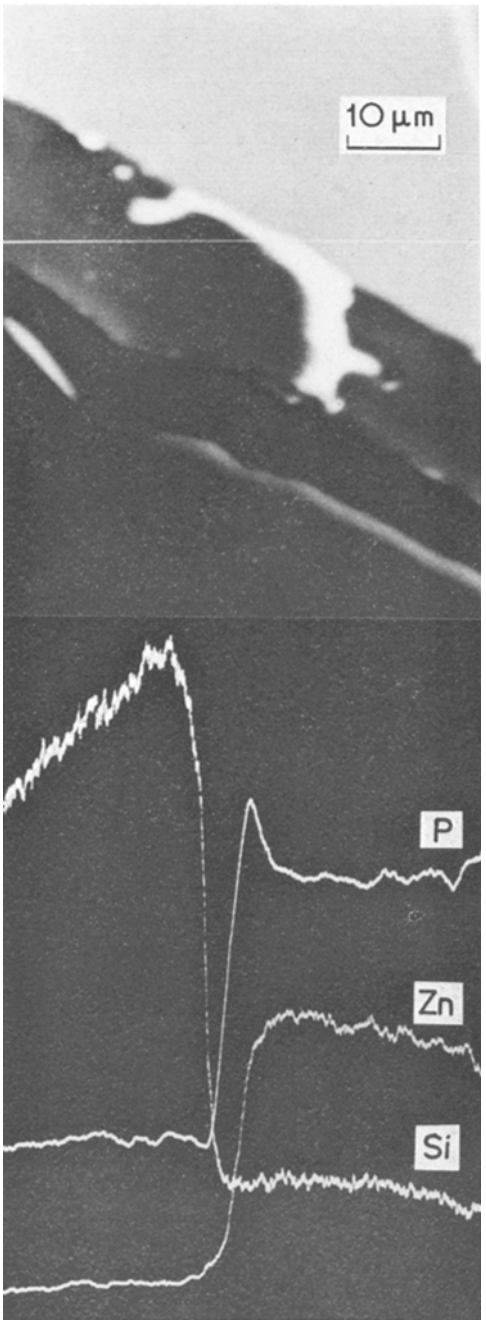

Figure 5 Electron image and composition profile (detected along the bright trace on the image) of a heterojunction cross section (using JXA-5 equipment). The upper part of the image is $ZnSiP_2$, the intermediate and outer Si layers are visible below.

The spacing of [010] lines is 0.037 μm in the $[10\bar{2}]$ direction, whereas that of the $[10\bar{2}]$ lines

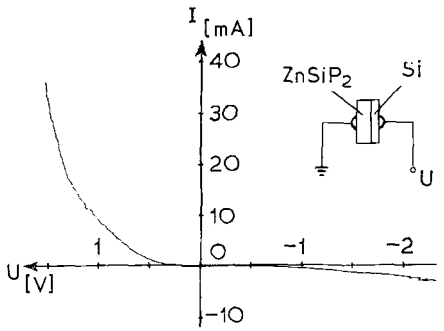

Figure 6 Current voltage characteristics of a Si-$ZnSiP_2$ n-n heterojunction.

is 0.095 μm in the [0 1 0] direction. The density of broken bonds amounts to $N_s = 4.76 \times 10^{13}$ cm^{-2}.

4. Discussion

The structural similarity of the $ZnSiP_2$ substrate and the Si layer together with some data reported on similar heteroepitaxial systems [4, 5] have suggested that a simple epitaxial relationship will take place, i.e. the corresponding identical cubic planes of the Si layer will lie parallel to the actual tetragonal substrate planes. (Strictly speaking, we can only say that these planes are nearly identical because of the tetragonal compression.) This suggestion proved to be valid for each of our investigated orientations.

It was not possible to determine with certainty the influence of the polar (1 1 2) and $(\bar{1}\,\bar{1}\,\bar{2})$ $ZnSiP_2$ planes on the deposition of the Si. The layer displayed on fig. 1 was most probably formed on the plane of lower chemical activity containing Zn and Si atoms, whereas on the opposite $(\bar{1}\,\bar{1}\,\bar{2})$ planes containing P atoms, Si layers of a complex structure with no regular growth patterns were observed.

In principle the (1 0 1) and (0 1 1) $ZnSiP_2$ planes should be covered by one type of atom. For III-V compounds it was estimated that the corresponding planes contain both types of atoms in substantially equal number, since there are no obvious strong natural forces to cause a particular type to appear preferentially on the surface. According to the existing analogies between the III-V and II-IV-V_2 compounds in other fields, it might be supposed that in the present case all three kinds of atoms will exist on the surface so the latter will form steps on an atomic scale. This complex surface structure might favourably affect the epitaxy by improving nucleation. This is in good agreement with the higher structural quality of the layers grown on (1 0 1) type $ZnSiP_2$ surfaces.

The heteroepitaxial Si layers contain numerous crystal defects, proved both by the indistinct reflections in the Laue patterns and by the lack of Kikuchi lines in the electron diffraction patterns. A considerable defect density was expected on the basis of the lattice mismatch and was confirmed by the misfit calculations based on the geometrical model. It is of interest to remark that for $ZnSiP_2$-Si the matching is more perfect than for the well-known Ge-Si heteroepitaxy.

Concerning misfit dislocations, there is an experimental evidence of $\langle 1\,1\,0 \rangle$ type misfit grid in the (1 1 1) type heterojunctions [8]. Therefore the misfit calculation may be corrected if precise experimental data will become available on the orientation of the misfit grid of the junction in question. It is supposed that the predicted geometrical model of the misfit grid will not be realised exactly due to the possible interactions between dislocations. These interactions can modify the directions and distances of misfit dislocations. Theoretically, they will not change the directions and magnitudes of the resultant Burgers vectors.

At the relatively high temperature of the growth, reaction occurred between the layer and the substrate. The microstructure showed the formation of an intermediate phase especially in the layers grown at higher temperatures. According to the phase diagram of the Si-P system [9] the appearance of a liquid phase in the temperature range of the layer growth is to be expected.

Due to the etching of the substrate, Zn and P are released and they can be incorporated in the growing layer. According to previous data the maximum solubility of Zn is 6×10^{16} cm^{-3}, whereas that of the P is 10^{22} cm^{-3}. Therefore, it is obvious that the latter will be dominant. This is in good agreement with the preliminary electrical measurements. For the exact interpretation of the electrical characteristics further investigations concerning the influence of the intermediate phase are necessary.

Acknowledgements

The author is much indebted to Professor N. A. Gorjunova (A.F. Ioffe Physico-Technical Institute, Leningrad) for suggesting the problem.

Acknowledgements are due to L. Varga for the X-ray data and the valuable discussions, to Mrs M. Farkas-Jahnke for the electron diffraction

measurements, to R. K. Vassel (Research Institute for Nonferrous Metals, Budapest) for EPMA. Thanks are also due to G. Stubnya and B. Szentpáli for their kind assistance.

References

1. A. S. BORSHCHEVSKII, N. A. GORYUNOVA, F. P. KESAMANLY, and D. N. NASLEDOV, *Phys. stat. sol.* **21** (1967) 9.
2. B. RAY, *J. Mater. Sci.* **3** (1967) 284.
3. N. A. GORYUNOVA, Proc. IX Int. conf. on the Physics of Semiconductors, Moscow **2** (1968) 1198.
4. A. S. BORSHCHEVSKII, *et al.* Processi rosta i structura monokristallicheskih sloev poluprovodnikov (NAUKA, Novosibirsk, 1968), p. 334.
5. A. J. SPRINGTHORPE, R. J. HARVEY, and B. R. PAMPLIN, *J. Crystal Growth* **6** (1969) 13.
6. A. J. SPRINGTHORPE and B. R. PAMPLIN, *ibid* **3, 4** (1968) 313.
7. D. B. HOLT, *J. Phys. and Chem. Solids* **27** (1966) 1053.
8. E. S. MEIERAN, *J. Electrochem. Soc.* **114** (1967) 292.
9. B. GIESSEN and R. VOGEL, *Z. Metallk.* **50** (1959) 275.

Received 14 July and accepted 10 September 1970.